Contents lists available at ScienceDirect

Chemical Engineering Research and Design

journal homepage: www.elsevier.com/locate/cherd

Biochar from olive mill solid waste as an eco-friendly adsorbent for the removal of polyphenols from olive mill wastewater

Nozha Abid[a,*], Mohamed Ali Masmoudi[a], Marwa Megdiche[a], Abdellatif Barakat[b], Mariam Ellouze[a], Mohamed Chamkha[a], Mohamed Ksibi[c], Sami Sayadi[d,**]

[a] Center of Biotechnology of Sfax, AUF (PER-LBP), BP: 1177, Sfax 3018, Tunisia
[b] UMR IATE 1208 CIRAD/INRA/Montpellier SupAgro/Université Montpellier, 2 Place Pierre Viala, Montpellier Cedex 5 34060, France
[c] Laboratory for Environmental Engineering and Eco-Technology, Sfax National School of Engineers, University of Sfax, BP: 1173, Sfax 3038, Tunisia
[d] Biotechnology Program, Center for Sustainable Development, College of Arts and Sciences, Qatar University, Doha 2713, Qatar

ARTICLE INFO

Article history:
Received 28 October 2021
Received in revised form 26 January 2022
Accepted 23 February 2022
Available online 26 February 2022

Keywords:
Olive mill wastewater
Adsorption
Olive mill solid wastes
Biochar
Polyphenolic compounds
Central composite design

ABSTRACT

In Tunisia, olive mill waste water (OMW) is discharged into evaporation ponds where they turn into solid waste (OMSW) and become a serious threat to the environment. This paper addresses for the first time how to valorize OMSW into a biochar (BC) that can be used as an adsorbent aiming at either the recovery or the removal of polyphenols from the OMW. In this work, BC was produced through the pyrolysis of OMSW. Response Surface Methodology (RSM) approach was used for optimization of the process parameters. Analysis of variance revealed that all four parameters (pH, adsorbent dosage, pyrolysis temperature and polyphenols loading) had a significant effect on the adsorption ($p < 0.05$). pH proved to be the most highly significant variable. The nonlinear Freundlich isotherm model was found to better describe the experimental adsorption process ($R^2 = 0.9911$), while maximum polyphenol adsorption at 30 °C was 140.47 mg/g. Indeed, OMW is known as a source of natural antioxidant such as Hydroxytyrosol. In this work, hydrxytyrosol proved to have a high adsorption affinity for the BC. Therefore, adsorption using BC is an appropriate technique that maximizes the recuperation of hydroxytyrosol. After detoxification, OMW is invested for a variety of applications.

1. Introduction

Olive oil which corresponds to one of the most highly appreciated vegetal oils in the world for its health benefits, has been produced at an average of 2.95 million tons per year (Doula et al., 2017). Unfortunately, its production has always had a negative side effect on the environment. Indeed, it has always resulted in the release of olive mill wastewater (OMW) estimated at an average of 30 million tons per year (Doula et al., 2017). Ducom et al. (2020) reported that 98% of this effluent was generated in the Mediterranean region. For instance, Tunisia, which was ranked the fourth international olive oil producer by the Food and Agriculture Organization (FAO) (FAOSTAT, 2014), was

* Correponding author at: Laboratory of Bioprocesses, Center of Biotechnology of Sfax, AUF (PER-LBP), BP: 1177, Sfax 3018, Tunisia.
** Correponding author.
E-mail addresses: nozha.abid@fss.usf.tn (N. Abid), ssayadi@qu.edu.qa (S. Sayadi).
https://doi.org/10.1016/j.cherd.2022.02.029

reported to have an average yearly discharge of this highly polluting effluent that is equal to 800,000 tons (C.O.I., 2017). Moreover, this waste presents a major environmental problem referring basically to the great values of chemical oxygen demand (COD) and biological oxygen demand (BOD) as well as the high load of phenolic compounds reaching values up to 25 g/L (McNamara et al., 2008). Multiple researchers emphasized that this effluent was responsible for several phytotoxic and antimicrobial effects (Aktas et al., 2001; El Hajjouji et al., 2007). From this perspective, there has been a spate of interest in the physico-chemical and biological processes for the treatment and valorization of this waste. Biological treatments were considered less expensive than physico-chemical ones and environmentally friendly (McNamara et al., 2008). However, the biological solutions like anaerobic digestion were affected chiefly by the inhibitory effect of the phenolic compounds on the activity of the microorganisms (Chen and Chen, 2009). Therefore, several researchers recommended to adopt integrated treatment processes based on pretreatments for polyphenol removal followed by biological processes (El-Gohary et al., 2009; Khoufi et al., 2006). Basically, polyphenol compounds are regarded as the main obstacle in the detoxification of OMW. However, this does not exclude that some of them correspond to high added value by-products like hydroxytyrosol (Tsagaraki et al., 2007). Thus, physical treatments including membrane technologies have been invested mainly for extraction of high added value by-products (Garcia-Castello et al., 2010). Unfortunately, this solution displayed some shortcomings, such as the limited membrane efficiency caused by the gelling substances contained in OMW and the high cost of the process (Garcia-Castello et al., 2010). Physical adsorption method onto activated carbon was widely applied for the phenolic compounds removal owing to its flexibility, simplicity of design and the large number of cavernous pores of activated carbon which provides a large surface area. Adsorption onto the activated carbons occurs between the physical or chemical bonds between adsorbate from the wastewater and the porous solid adsorbent. Recently, numerous studies have focused on biochar (BC). It is a carbon-rich material, produced by controlled combusting under insufficient oxygen levels of a variety of biomass materials (Cantrell et al., 2012). BC drew much attention as an alternative to activated carbon, in view of its low cost (Hu et al., 2020). Indeed, it represents an ecofriendly product since it is produced from organic wastes and is being used for pollutants removal through adsorption and/or for soil improvement. For adsorption applications, the sorption capacity of BC proved to depend on pyrolysis temperature, residence time and reaction atmosphere (Li et al., 2018) as well as material properties (Chen and Chen, 2009). Indeed, a wide variety of waste biomasses was converted into BC such as rice straw, bagasse, poplar wood, bamboo and swine solids (Li et al., 2018). By adopting univariate optimization, prior works have reported the adsorption behavior of phenolic compounds from OMW (Achak et al., 2009; Senol et al., 2017; Stasinakis et al., 2008). However, as was highlighted by Lima et al. (2007), this strategy requires numerous variable experimental runs which are time-consuming and costly. In addition, it wrongly considers the variables totally independent of each other. Therefore, it fails to depict the interactive effects of different factors on the adsorption process. To overcome such limitations, statistical experiment design methods need to be considered. On the other side, despite the huge efforts dedicated by researchers and the accomplished progress in OMW treatment, there was no totally satisfactory sustainable approach adopted for OMW treatment. Thus, this waste continued to be stored in storage ponds where it progressively turned into olive mill solid wastes (OMSW). So far, this new waste has received little attention from researchers in spite of its highly polluting effect. For this reason, an integrated and innovative process has been conceived by our research group aiming at the development of a cost-effective and sustainable approach for the management and valorization of OMW and OMSW in a circular economy concept. Briefly, OMSW is treated through pyrolysis process, generating bio-oil used as energy carriers and biochar which can be used as polyphenols adsorbent or soil improver. Thus, adsorption treatments would detoxify OMW by polyphenol elimination in view of their recovery as high-added products like hydroxytyrosol. Subsequently, detoxified OMW could be post-treated anaerobically. The present study represents a primary step towards achieving our objectives. Specifically, it purported to achieve the following targets. Firstly, it attempted to carry out a conversion of OMSW from Tunisian evaporation ponds into BC through slow pyrolysis. Secondly, BC was subjected to morphological and structural characterization using several techniques such as elemental analysis (CHNS), Fourier transform infrared spectroscopy (FTIR) and scanning electron microscopy (SEM). Thirdly, central composite design (CCD) was conducted to optimize the performance of sorption biochar and assess the significance of various parameters such as pH of the solution, initial polyphenols concentration (or dilution), pyrolysis temperature and adsorbent dosage. Fourthly, the nonlinear Langmuir and Freundlich isotherms models were performed to predict OMW polyphenols adsorption. Finally, selective removal of hydroxytyrosol was investigated.

2. Materials and Methods

2.1. Raw materials

Raw OMW employed in this study was produced by a continuous olive oil mill located in Sfax (Tunisia). OMSW samples were collected from open evaporation ponds in Agareb, Sfax, Tunisia.

2.2. OMW pretreatment

Due to the high total suspended solids content of OMW, samples were centrifuged by Universal 320 R at 6000 tr/min for 10 min in order to separate suspended solids before use.

2.3. Physicochemical analysis and phytotoxicity test of OMW

The samples were weighed before and after being oven-dried at 105 °C to measure their total solids content. Next, they were calcinated at 550 °C for 2 h to determine the mineral matter. To determine the total suspended solids, the samples were centrifuged at 4000 rpm for 20 min. Subsequently, the retained residues were dried at 105 °C. Total chemical oxygen demand (COD) was analyzed according to the standard procedure following the American Public Health Association (APHA, 2012). Biological oxygen demand (BOD_5) was determined by the manometric method. Kjeldahl digestion and distillation method were used to determine Kjeldahl nitrogen (Kj-N). Total polyphenol compounds (PC) were quantified using the Folin-Ciocalteu assay, as described by Aliakbarian et al. (2015). Total phosphorus was analyzed using ammonium molybdate spectrophotometric method. Quantification and identification of phenolic monomers were carried out by means of HPLC analysis performed in a Shimadzu apparatus with a C-18 column. Mineral and metal analyses were also performed by service Laboratory (CITET, Tunisia). The samples were analyzed using inductive coupled plasma- atomic emission spectroscopy (ICP-AES). OMW phytotoxicity was assessed by a seed germination index assay using *Lepidium sativum* according to Zucconi et al. (1981).

2.4. Biochar preparation

To eliminate any contamination, OMSW was washed with distilled water. After drying at 40 °C for 48 h, the aggregates were crashed and the particles were sieved through a 1 cm sieve. The pyrolysis experiments were conducted into a cylindrical reactor under controlled oxygen conditions, locally fabricated. OMSW upload per experiment was 150 g, with a residence time of 30 min at a specified pyrolysis temperature. Three pyroly-

sis temperatures were tested 450 °C, 550 °C and 650 °C with heating rates of 10 °C/min. Nitrogen, as a gas flow, was sparging with a flow rate of 1 L/min. The obtained biochars were rinsed with distilled water to return impurities before oven-drying at 80 °C for 24 h. Afterwards, the fraction with particle size 6 < mesh < 8 was retained and stored in glass vials for subsequent works.

2.5. Biochar characterization

pH was determined according to the method used by Hmid et al. (2014). The yield was expressed as a dry weight percentage of the starting OMSW.

Ash content was determined based on the method used by Peng et al. (2011) after combustion in a muffle furnace at 750 °C for 6 h. Microscopic morphology of the adsorbent was analyzed by scanning electron microscopy (SEM) using JEOL(JSM 5400). Fourier transform infrared spectroscopy (FTIR) was employed to determine the functional groups present on the surface of the biochars (Nicolet 380 FTIR). The CHNS composition was determined using aVario Micro V4.0.2 elemental analyzer (Elementar®, Germany). The O composition was determined using a Vario MicroV3.1.6 elemental analyzer (Elementar®, Germany). Point of zero charge, pH_{pzc}, was conducted according to the method used by Bouzid et al. (2008). The specific surface area, pore volume, pore diameter and pore size distribution of the BC were measured by sorption analyses with N_2 at −196 °C using a Micromeritics ASAP 2020 analyzer.

2.6. Adsorption experiments

Batch method experiments were conducted in erlens with 100 mL of pretreated OMW. A rotary shaker was used for solutions agitation at 200 rpm and 30 °C using a thermoregulator. Univariate experiments were performed using various adsorbent dosages (1, 5, 10, 15, 20 and 25 g/100 mL), pH values (2–12), OMW dilutions (1/3 and 1/5) and pyrolysis temperatures (450 °C, 550 °C and 650 °C). At predefined time intervals, the BC was separated from the samples of 1 mL using millipore membrane filters of 0.2 μm before determining residual concentration of total polyphenols following the same protocol previously described by Aliakbarian et al. (2015). Polyphenols amount of adsorption at equilibrium, q_e (mg/g) or at time t, q_t (mg/g) was calculated in terms of the subsequent equations:

$$q_e = \frac{(C_0 - C_{eq})\,V}{X} \quad (1)$$

$$q_t = \frac{(C_0 - C_t)\,V}{X} \quad (2)$$

The PC removal (%) at time t was computed as follows:

$$\text{PC removal} = \frac{(C_0 - C_t)}{C_0} \times 100 \quad (3)$$

where C_0 and C_{eq} are the initial and equilibrium concentration of PC (mg/L) respectively; C_t is the concentration of PC at time t; V is the volume of solution (L) and X is the mass of dry adsorbent (g).

Besides, experimental conditions followed for the adsorption isotherm were: a temperature of 30 °C, a pH of 12, an adsorbent dosage of 2 g/100 mL, a contact time of 24 h and polyphenols concentration ranging from 470 to 3400 mg/L.

To investigate the best-fit model for the kinetic studies and adsorption equilibrium, the determination coefficient (R^2), chi squared (χ^2) value and the residual root-mean-square error (RMSE) were applied according to the following equations (Parsa et al., 2019):

$$R^2 = 1 - \frac{\sum(q_{e,exp} - q_{e,cal})^2}{\sum(q_{e,exp} - q_{e,mean})^2} \quad (4)$$

$$\chi 2 = \sum \frac{(q_{e,exp} - q_{e,cal})^2}{q_{e,cal}} \quad (5)$$

$$RMSE = \sqrt{\frac{1}{n-p}\sum_{i=1}^{n}(q_{e,exp-}q_{e,cal})_i^2} \quad (6)$$

where $q_{e,exp}$ (mg/g) is the amount of PC uptake at equilibrium; $q_{e,cal}$ (mg/g) is the amount of PC uptake obtained from the models and $q_{e,mean}$ (mg/g) is the mean of the $q_{e,exp}$ values'; n is the number of experimental data and p is the number of parameters within model equation. Equilibrium and kinetic models were fit by utilizing the nonlinear fitting method applying the software program Mathematica 9.

2.7. RSM experimental design

Polyphenols removal efficiency was optimized using CCD with the centered face using four independent variables, namely adsorbent dosage (A), pH (B), pyrolysis temperature (C) and initial polyphenols concentration (D). Table S1 (Supplementary data) portrays experimental parameters levels. CCD requires 16 factorial runs with 6 central runs and 8 star points as was recommended by Bajpai et al. (2012). All experiments, with 30 runs, were conducted according to the CCD matrix (Table S2) and were analyzed with Design Expert 11.

The adequacy of the predicted model was checked through the analysis of variance (ANOVA) that evaluated the regression coefficient (R^2), the lack of fit and the Fisher test value (*F-value*) at a significant level of 0.05. In order to estimate the optimal conditions of adsorptions, three dimensional (3D) response surface was constructed. The function of desirability was used by fixing a maximum target of percentage removal of PC so as to perform the optimization of the parameters.

3. Results and Discussion

3.1. OMW characterization

Table 1 reveals the main properties of raw OMW and pretreated OMW. To start with, the raw OMW displayed an acidic pH value and a high electric conductivity. But more importantly, its BOD_5 value of 7.75 g/L was much lower than that of COD (68.35 g/L). Moreover, germination index value of *Lepidium sativum* was equal to 0%. This can be attributed to the presence of phenolic compounds (5 g/L) which are responsible for several antimicrobial and phytotoxic effects as well as toxic fatty acids (Aktas et al., 2001; El Hajjouji et al., 2007; Sayadi et al., 2000). Hence in total agreement with Khoufi et al. (2009), it could be inferred that raw OMW had a low biodegradability and a high toxicity. To remove total suspended solids, a pretreatment was undertaken, which seemed to affect some of the physicochemical characteristics of OMW (Table 1). Indeed, its total suspended solids dropped to 0.5 g/L. Likewise, there

Table 1 – Physicochemical characteristics and phytotoxicity test of raw OMW and pretreated OMW.

Parameters	Raw OMW	Pretreated OMW
pH	5 ± 0.06	4.9 ± 0.05
Electrical conductivity (mS/cm)	14.4 ± 0.1	14,7 ± 0.1
Total solids (g/L)	55.3 ± 0.43	42.6 ± 0.46
Mineral matter (g/L)	12.4 ± 0.1	12.3 ± 0.23
Total suspended solids (g/L)	10.6 ± 0.2	0.5 ± 0.03
Total COD (g/L)	68.35 ± 1.76	47.4 ± 2.8
BOD_5 (g/L)	7.75 ± 1.2	1.75 ± 0.07
PC (g/L)	5 ± 0.13	3.4 ± 0.12
Kj-N (g/L)	0.77 ± 0.04	0.3 ± 0.06
Germination index (%)	0	20 ± 1.5

Data are represented by mean ± standard deviation.

Table 2 – Physicochemical and surface structures of the biochars produced at a pyrolysis temperature of 450 °C and 650 °C.

Parameters	Biochar produced at 450 °C	Biochar produced at 650 °C
pH	10.8 ± 0.05	11.1 ± 0.04
Ash contents (%)	29 ± 2.26	34.2 ± 1.51
Yield (%)	29.2 ± 2.7	27.4 ± 1.1
pH_{pzc}	8.7	9.7
C (db%)	45 ± 2.8	48.8 ± 1.8
N (db%)	2.45 ± 0.13	1.9 ± 0.1
H (db%)	2.26 ± 0.05	0.97 ± 0.04
S (db%)	1.23 ± 0.32	0.85 ± 0.11
O (db%)	19.47 ± 0.3	15.3 ± 0.4
Atomic ratio O/C	0.32	0.23
Atomic ratio H/C	0.6	0.24
Atomic ratio (O + N)/C	0.37	0.27
Surface structure		
BET surface area (m^2/g)	2.77	6.39
Pore size (nm)	13.42	15.33
Pore volume (cm^3/g)	0.009	0.0245

Data are represented by mean ± standard deviation.
db: oven dry basis.

was a decrease in its COD, BOD_5, total solids, PC and Kj-N. This was accompanied by a slight increase in germination index which rose to 20%.

3.2. *Biochar characterization*

The original OMSW was slightly acidic (pH 6.2). It had a high electrical conductivity (18.2 mS/cm) and a high ash content (20.1%). Table 2 highlights the main properties of the BC produced at 450 °C and 650 °C. Both materials were alkaline and pH value of BC produced at 450 °C was lower than the one produced at 650 °C. Our result is very close to previous findings reported by Hmid et al. (2014) and Hanandeh et al. (2016) who obtained the respective alkaline pH values of 9.7 and 10.2 for BC derived from olive mill wastes pyrolized at 430 °C and 450 °C, respectively. Biochars corresponding to pyrolysis temperature of 450 °C and 650 °C had yields of 29.2 % and 27.4 % respectively. This result was in good accordance with the findings of Abdelhadi et al. (2017) about biochars derived from olive mill solid wastes having yields ranging between 24 and 35% of the biomass. The ash contents and pH_{pzc} of BC increased with increasing pyrolysis temperature. Points of zero charge were alkaline with pH_{pzc} of 8.7 and 9.7 for BC produced at 450 °C and 650 °C respectively (Fig. S1). This was also close to the alkaline pH_{pzc} value of 9.46 reported by Martín-Lara et al. (2019) in their investigation on BC of carbonaceous materials from olive cake obtained by slow pyrolysis at 450 °C. Compared to BC produced at 450 °C, C contents were higher for BC produced at 650 °C but the contents of N, O, H and S were lower. Consequently, the H/C, O/C and (O + N)/C decreased with increasing temperature. The BC produced at 450 °C and 650 °C had values of atomic ratio (N + O)/C of 0.37 and 0.27 respectively. When compared to the BC derived from a three-phase OMW pyrolized at 480 °C (Hmid et al., 2014), or the one derived from olive cakes pyrolized at 450 °C (Martín-Lara et al., 2019) with (N + O)/C ratios of 0.12 and 0.19 respectively; the result obtained in this study would be considered as high values. This finding reveals the polar nature of the BC since (N + O)/C ratio was used as an index for surface polar functional groups (Zhang et al., 2011). Ferri et al. (2011) confirmed that this polar nature was responsible for the adsorption efficiency of phenolic compounds from OMW. The biochar pyrolized at 450 °C had a small BET surface area of 2.77 m^2/g and a pore diameter of 13.42 nm. Therefore, it can be classified as a mesoporous material (between 2 and 50 nm). Both biochars pyrolized at 450 °C and 650 °C exhibited a pore size distribution from 1.88 nm to 187 nm (Fig. S2). By increasing the pyrolysis temperature to 650 °C, the mesopore volume increased by about 3 folds. Thus, we can conclude that increasing carbonization temperature to 650 °C enhanced mesoporosity. Considering phenol molecular size (0.46–0.54 nm), the high mesopores fraction would play an important role in adsorption especially in OMW containing polyphenols of different molecular sizes.

The SEM micrograph of the OMSW (Fig. 1a) had a rough surface with no pores. In contrast, Fig. 1b, presenting the SEM micrograph of the BC pyrolized at 450 °C, demonstrates the existence of visible pores. The particles surfaces were grainy and rough owing to the presence of tubular and elongated shapes while the pore sizes were not uniform. Additionally, Fig. 1c showing the SEM micrograph of the BC pyrolized at 650 °C, displays more visible pores all over the surface. Finally, Fig. 1d showing the SEM micrograph of the BC pyrolized at 650 °C after adsorption, reveals that the sorbent surface was partially affected by the adsorbed compounds due to the sample heterogeneity.

The FTIR analysis of OMW and biochar pyrolized at 650 °C before and after adsorption is reported in Fig. 2.

Resting on spectrum a of OMW, the band at 1633 cm^{-1} is associated with the C=C in aromatic ring (Tran et al., 2018). Similarly, the band at 3264 cm^{-1} is related to (O—H) stretching vibrations in hydroxyl groups in alcohols and phenols as was interpreted by Tran et al. (2018) and Hafidi et al. (2005). This result goes in good conformity with previous findings reported by El Hajjouji et al. (2007), which are related to the analysis of Moroccan OMW generated by the three-phase centrifugation technique.

Spectrum b shows the BC pyrolized at 650 °C before adsorption. The bands at 866 cm^{-1} results from an out of plane bending mode of aromatic C—H (Tran et al., 2018). The band at 1025 cm^{-1} refers to stretching C—O groups (Yang and Lua, 2003). The band assigned at 1104 cm^{-1} would correspond to C—O stretching as was interpreted by Yang and Lua (2003). Furthermore, the band at 1379 cm^{-1} is associated with the C—H bending vibration of the methyl group. Finally, the band at 2918 cm^{-1} is related to the aliphatic C—H stretching (Tran et al., 2018).

Spectrum c indicates the BC produced at 650 °C after OMW adsorption. It could be easily noticed that new bands at 3264

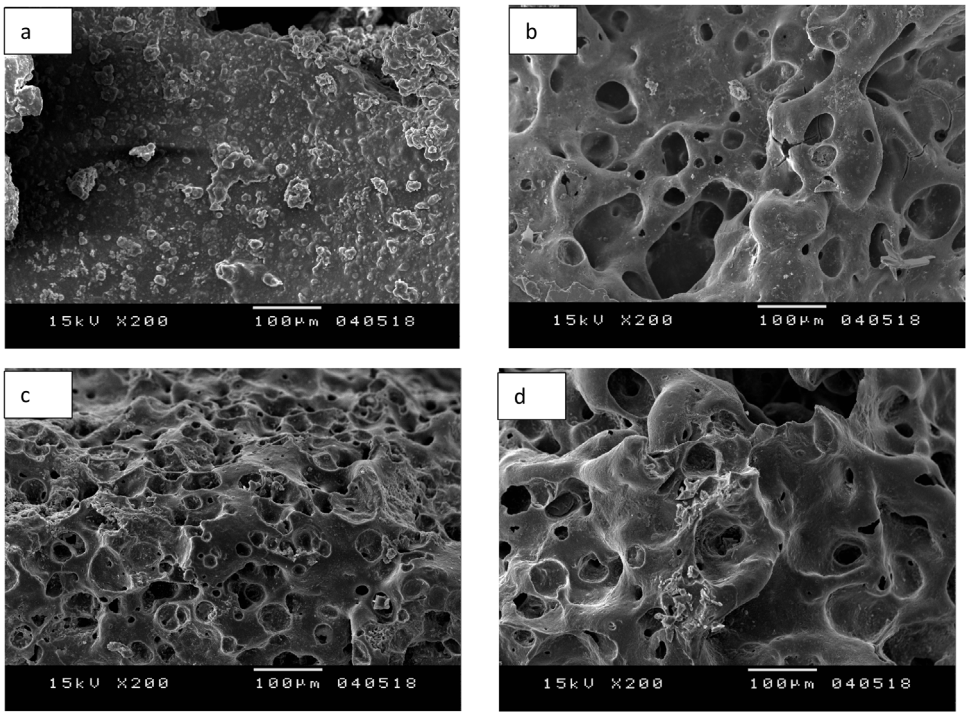

Fig. 1 – SEM micrographs of (a) OMSW, (b) BC pyrolized at 450 °C, (c) BC pyrolized at 650 °C and (d) BC pyrolized at 650 °C after adsorption.

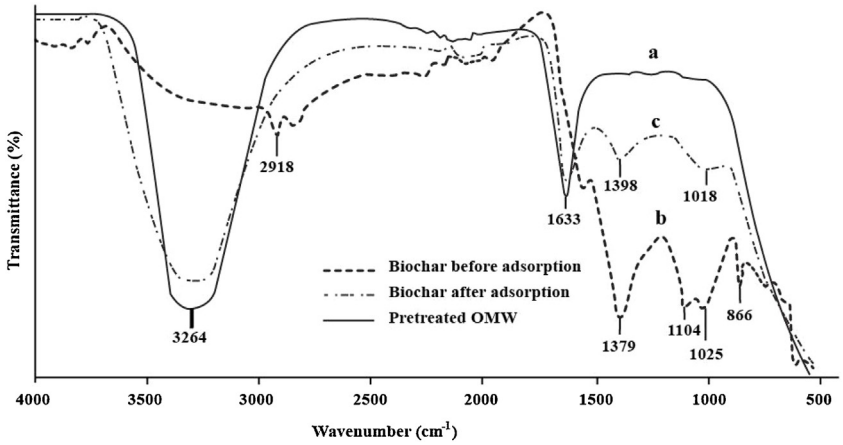

Fig. 2 – FTIR spectra of (a) pretreated OMW (b) BC produced at 650 °C before adsorption and (c) BC produced at 650 °C after OMW adsorption. (Conditions: pH = 12, adsorbent dosage = 15 g/100 mL and initial PC = 3400 mg/L).

cm^{-1} and 1633 cm^{-1} appeared. They are related to (O—H) stretching vibrations in hydroxyl groups in phenols and to the C=C in aromatic ring, respectively. These results indicate the presence of polyphenols and confirm that these compounds are adsorbed onto BC. Spectrum c indicates also that some bands shifted to different wavenumbers. Notably, the C—O groups shifted from 1025 cm^{-1} to 1018 cm^{-1} and C—H bending vibration of the methyl group shifted from 1379 cm^{-1} to 1398 cm^{-1}. The bands at 866 cm^{-1}, 1104 cm^{-1} and 2918 cm^{-1} disappeared. The shift and alteration in band height of 1025 cm^{-1} and disappearance of vibration band of 1104 cm^{-1} which are related to C—O groups after adsorption would signify the involvement of oxygen sites in polyphenols adsorption (Dąbrowski et al., 2005). This would confirm the finding of Liu et al. (2011) corroborating that the mechanism of adsorption may involve interaction of the oxygen containing functional groups with phenols via chemical interactions such as hydrogen binding.

3.3. *Sorptive properties of Biochar*

3.3.1. *Effect of contact time*

Both removal efficiency (Fig. 3a) and adsorption capacity (qe) (Fig. 3b) increased with the increase of contact time until 12 h. This may refer to the availability of vacant surface sites of the BC leading to fast adsorption of the OMW polyphenols. Beyond 12 hours of contact time, the percentage of polyphenols removal and the adsorption capacity remained almost unchanged referring to the slow pore diffusion of polyphenols into the adsorbent. Furthermore, the sorption efficiency decreased owing to the electrostatic repulsion between the polyphenols adsorbed on the BC surface and the sorbate species available in the solutions (Ferri et al., 2011; Senol et al., 2017). After equilibrium, about 40% of total polyphenols were adsorbed (Fig. 3a). No desorption phenomena were recorded as those noticed in using dried olive pomace as polyphenols OMW adsorbent (Stasinakis et al., 2008). Fur-

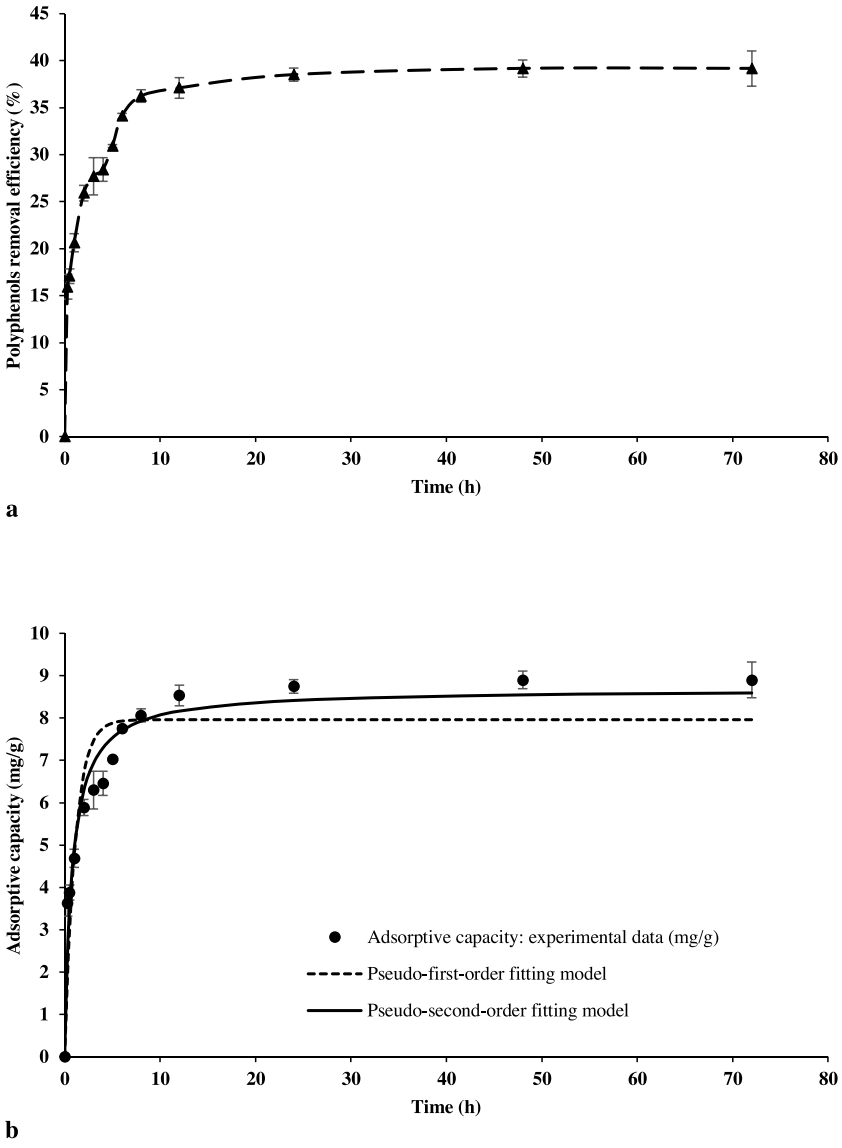

Fig. 3 – (a) Effect of contact time on polyphenols removal in pretreated OMW. (b) Kinetic models for OMW polyphenols removal. (Conditions: adsorbent dosage = 15 g/100 mL; pH = 5; initial polyphenols concentration = 3400 mg/L and pyrolysis temperature = 650 °C).

thermore, this result goes in tandem with the observation of Galiatsatou et al. (2002) about the adsorption of total OMW phenols into a series of activated carbons derived from olive stones and olive pulps. These researchers argued that this adsorbent reached equilibrium between 1 h and 22 h. Finally, a relatively faster adsorption on commercial activated carbons was previously recorded by Senol et al. (2017) and Aliakbarian et al. (2015) who asserted that the adsorption of polyphenols from OMW required a contact time up to 10 min and 120 min, respectively.

In order to elucidate the adsorption mechanism for polyphenols sorption onto BC, both of the pseudo-first order equation (Eq. 7) and the pseudo-second order equation (Eq. 8), were applied to the data. These equations are presented as follows:

$$q_t = q_e\,(1 - e^{-k_1 t}) \tag{7}$$

$$q_t = \frac{q_e^2\, k_2\, t}{1 + k_2 q_e\, t} \tag{8}$$

Table 3 – Kinetic parameters calculated by the two kinetic models.

Model	Parameters		$q_{e,\,exp}$ (mg/g)
Pseudo-first- order	k_1 (1/h)	0.913	8.9
	q_e (mg/g)	7.9655	
	χ^2	2.7864	
	RMSE	0.9574	
	R_1^2	0.8717	
Pseudo-second-order	k_2 (g/mg h)	0.1505	
	qe (mg/g)	8.6791	
	χ^2	0.9065	
	RMSE	0.5497	
	R_2^2	0.9577	

where q_e and q_t (mg/g) are the amounts of adsorbed phenolic compounds at equilibrium and at any time, respectively; k_1 (h^{-1}) is the equilibrium rate constant of the pseudo-first order equation and k_2 (g/mg h) is the rate constant for pseudo-second order equation.

The kinetic data obtained from nonlinear regression analysis fitting are presented in Fig. 3b. Table 3 illustrates the

nonlinear-fitting results of both kinetic models to the experimental data.

According to Table 3, pseudo-second model exhibited higher R^2 ($R_2{}^2 = 0.9577$) and lower χ^2 and RMSE values than pseudo-first model. In addition, qe value calculated from pseudo-second model (8.6791 mg/g) was closer to the experimental q_e (8.9 mg/g) than the one calculated from pseudo first model (7.9655 mg/g). These findings denoted that the kinetics of phenolic compounds adsorption in this study follows better the second order model. Thus, it can be assumed that the rate-limiting step of polyphenols adsorption may be chemical sorption (Ho and McKay, 1999). This may stipulate that for PC adsorption, exchange reactions occur between PC and adsorbent surface up to the occupancy of all surface functional sites. Then, the diffusion of PC in the BC network would lead to other types of interactions such as hydrogen phobic interaction and hydrogen bonding.

The linear pseudo-second-order kinetic model was highlighted by Stasinakis et al. (2008) and Aliakbarian et al. (2015) during OMW polyphenols adsorption onto olive pomace and activated carbon respectively.

3.3.2. *Effect of pyrolysis temperature*

Fig. 4a illustrates the effect of pyrolysis temperature on the polyphenols removal under the following experimental conditions: adsorbent dosage = 5 g/100 mL; pH = 5 and initial polyphenols concentration = 3400 mg/L. The removal of polyphenols from OMW increased slightly from 23.8% at pyrolysis temperature of 450 °C to 26.6% at 650 °C. This could be attributed to the fact that the higher pyrolysis temperature generated a higher porosity. This finding corroborates the one obtained through the above SEM micrograph analysis. In addition, it confirms previous results reported by Sanginés et al. (2015) on slow pyrolysis of olive stones.

3.3.3. *Effect of BC dosage*

Fig. 4b depicts the effects of BC dosage on the removal of polyphenols under the following experimental conditions: pH = 5; initial polyphenols concentration = 3400 mg/L and pyrolysis temperature = 450 °C. As can be detected, the removal efficiency increased from 12.4% to almost 40% as the adsorbent dosage increased from 1 to 15 g/100 mL. This would be assigned to the creation of more adsorption sites as a consequence of the increase of surface area. However, beyond this adsorbent dose, the removal efficiency seemed to remain practically constant. This phenomenon may be explained by the fact that the ratio of polyphenol molecules to the vacant adsorbent sites decreased as the adsorbent dosage increased, thus leading to polyphenols bonding to the surface sorbent. Subsequently, an equilibrium between adsorbent and unadsorbed molecules would be established restraining the sorption process (Achak et al., 2009; Senol et al., 2017). These findings go in good agreement with the assertions of Senol et al. (2017) in their study of OMW with an initial polyphenols content of 4821.5 mg/L. These scientists emphasized that surface active sites of the commercial activated carbon reached saturation beyond the addition of 5 g/100 mL. The adsorptive capacity (mg/g) was evaluated between the different dosages (Fig. S3). It was high at low adsorbent dosage and decreased as the amount of adsorbent increased. When the adsorbent dosage increased from 5 to 15 g/100 mL, the adsorptive capacity was dropped by 47.8% while about 56 % of increase in the removal efficiency was reached (Fig. 4b). The most important factor which contributes in reducing the adsorption capacity at high adsorbent dosage is that the target sites remain unsaturated (Han et al., 2006).

3.3.4. *Effect of pH*

Fig. 4c illustrates the behavior of BC in the presence of a pH ranging between 2 and 12. The experimental conditions were: adsorbent dosage = 5 g/100 mL; initial PC = 3400 mg/L and pyrolysis temperature = 450 °C. At pH 2, total phenols removal was about 28.4% and remained almost stable up to pH 5. Afterwards, it increased gradually until reaching 45% at pH 12. These findings go in good conformity with those of Stasinakis et al. (2008) as well as those of Achak et al. (2014, 2009) concerning OMW polyphenols removal on combusted olive pomace, wheat bran and banana peel, respectively.

The effect of pH on adsorption of phenolic compounds was considered by Mondal et al. (2016) and Quast (2018) depending on the ionization constant (pKa) of the phenolic compounds as well as pH_{pzc} of the adsorbent. Indeed, Xiaoli and Youcai (2006) argued that when pH is equal to pKa, the neutral and anion forms are equal. Ahmaruzzaman and Sharma (2005) added that when pH is lower than pKa, phenolic compounds are basically in the neutral molecular form. However, when pH is higher than pKa, the compounds are predominantly in the form of phenolate species.

This study revealed that the pH_{pzc} of the BC was equal to 8.7 indicating that surface adsorbent would have a negative charge at pH above 8.7. On the other side, phenol would dissociate into anionic forms at pH above 9.89. In such a condition and according to Haghseresht et al. (2002), a decrease in phenol adsorption efficiency occurred at pH 12 owing to electrostatic repulsion. However, this explanation would be relevant for the single polyphenol component, with a known pKa (Mohammed et al., 2018). Therefore, pH mechanism in this work cannot be reduced only to the degrees of ionization of PC and adsorbent surface charge as decisive factors. Many surface phenol interactions in addition to electrostatic ones may have notable contributions. The role of pH on polyphenols adsorption was lately reviewed by Lawal et al. (2020) who demonstrated that for the phenolate adsorption, negative charge-assisted hydrogen bonding was likely to be the main adsorption mechanism.

Consequently, it can be concluded that with the rise of pH values at 11 or 12, most of the PC would be in the form of phenolates while the surface BC would become negatively charged. Hence, as was explained by Lawal et al. (2020), the sorption capacity probably increased via hydrogen bonding.

Moreover, as was clarified by Achak et al. (2014), because of the heterogeneity of the BC surface, positively charged groups may exist and surface phenol interaction via electrostatic attraction would occur. Finally, the relative reduced PC removal at low pH could be assigned to additional protons, introduced by acid solution in the OMW solution, which competed with phenolics ions for surface adsorption (Dąbrowski et al., 2005).

3.3.5. *Effect of initial polyphenols concentration*

Fig. 4d presents the effect of initial polyphenols concentration on the removal of polyphenols respecting the following conditions: adsorbent dosage = 5 g/100 mL; pH = 5 and pyrolysis temperature = 450 °C. The polyphenols removal efficiency increased gradually from about 24.5% to 38.2 % with the decrease of the initial polyphenols concentration represented by a 5-time water dilution of OMW. This observation goes in total agreement with the findings reported by Habib Dakhil (2013) on phenol adsorption using sawdust and the observa-

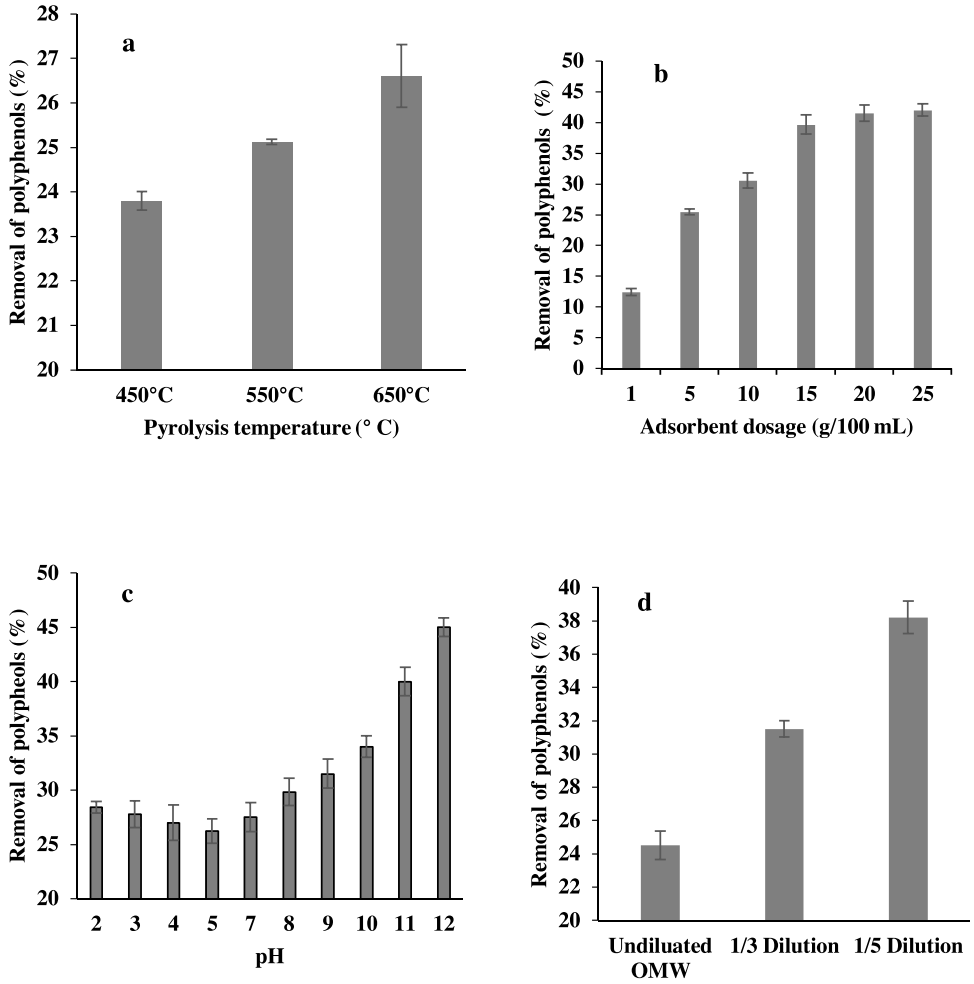

Fig. 4 – Effect of pyrolysis temperature (a), adsorbent dosage (b), pH (c) and initial polyphenols concentration (d) on the removal of polyphenols.

tions enacted by Ekpete et al. (2010) on phenol adsorption using commercial activated carbon. Both researchers emphasized that the surface saturation depended on the initial phenol concentration. In other words, as the initial phenol concentration increased, the accumulation of phenolic compounds on the surface caused a decrease in percentage removal. These findings go in good consistency with results obtained previously by Petrotos et al. (2016) and Senol et al. (2017) who investigated OMW adsorption on the macroporous resin and activated carbon, respectively.

3.4. *Process modeling*

3.4.1. *Statistical analysis*

The experimental design and results dealing with the optimization by response surface methodology are presented in Table S2.

The following second-order polynomial model equation was found after fitting obtained experimental results to the quadratic regression model. It is expressed with respect to coded variables.

$$\text{Polyphenolremoval}(\%) = 32.60 + 6.04A + 8.49B + 0.8978C - 4.57D - 3.20A.B - 1.01A.D + 3.58A^2 + 4.80B^2 + 4.38D^2 \quad (9)$$

For ANOVA analysis of the polyphenols removal efficiency (Table S3), solely the statistically significant terms were incorporated into the final response regression models so as to achieve a good fit. This analysis reveals two important results. Firstly, the *F* value of 386.94 with a probability < 0.0001 would prove that the model was significant, whereas the insignificant lack of fit ($F = 1.7$, $p = 0.29$) demonstrated that the *F*-statistic was inconsequential, which implies adequate accordance between the process variables and final responses. Secondly, the R^2 value of 0.9943 and that of 0.9917 for the adjusted R^2, being both close to 1, would imply reasonable agreement between the experimental and the predicted values. The coefficient of variance value of 2.48, being <10, would imply that the data were accurate. The relationship between predicted data and actual data of PC adsorption is displayed in Fig. S4. It is noteworthy that there was an adequate fitness between experimental and predicted data. Finally, the *p* value < 0.0001 and the $F = 1297.71$ related to the pH solution would imply that pH had the most significant effect on PC removal. The second effective parameter would be the adsorbent dosage (*p* value < 0.0001; *F* value = 657.01). Then, the third effective parameter would be the initial PC concentration (*p* value < 0.0001; *F* value = 375.94). The last parameter, corresponding to pyrolysis temperature, would have less significant effect on the response with a *p* value = 0.0011 and an *F* value = 14.53. It could be deduced that this finding was

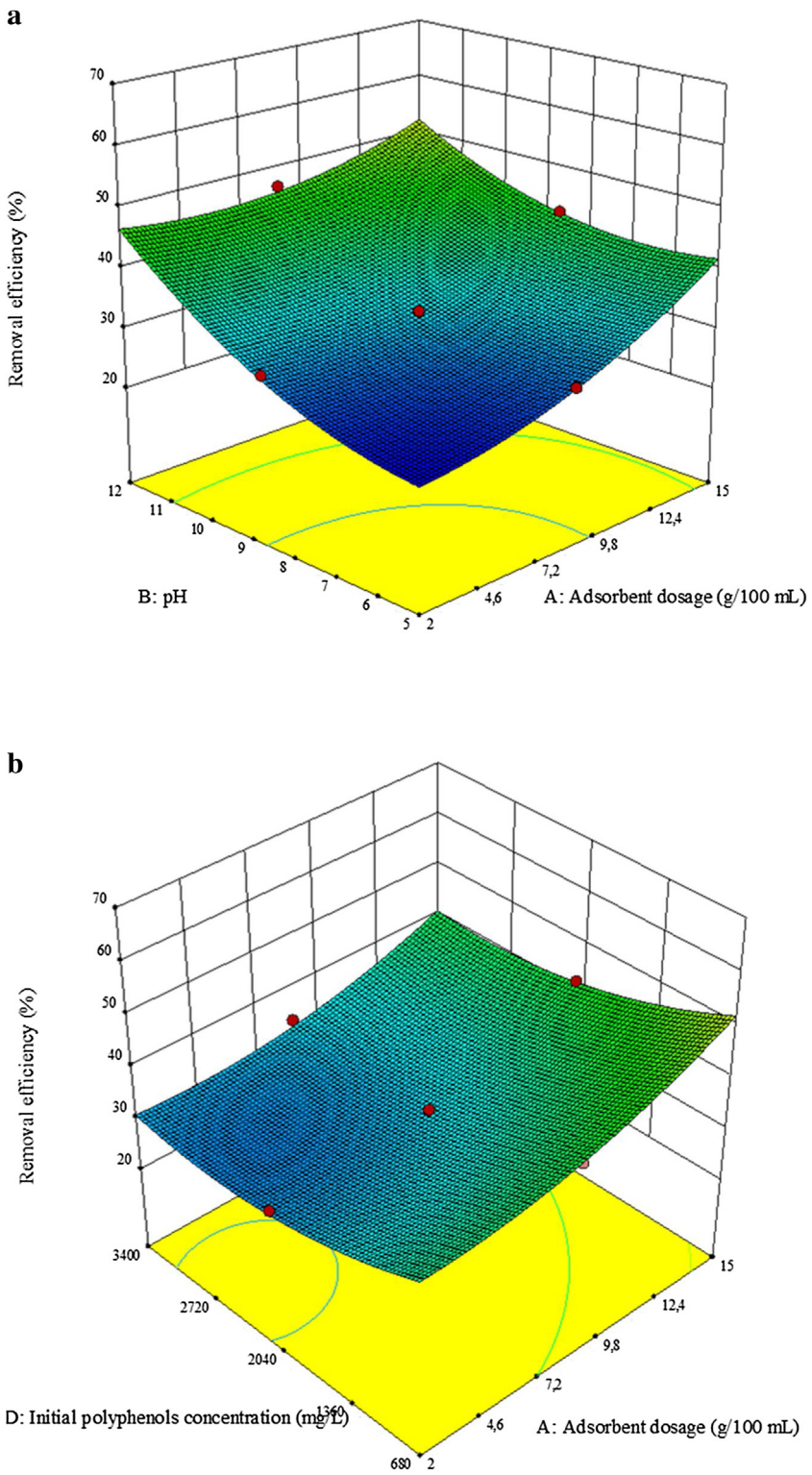

Fig. 5 – 3D response surface plots of the combined variables effect on polyphenols removal efficiency: (a) interaction between pH and adsorbent dosage (b) interaction between adsorbent dosage and initial PC concentration.

of a great importance because the highest significant effect of pH revealed by CCD method could not be detected by the univariate experiments (Achak et al., 2014, 2009; Senol et al., 2017). In addition, these findings corroborate the assertion of Dąbrowski et al. (2005) that solution pH affects the surface charging whose role dominates even in comparison with porosity distribution in solid adsorbents.

3.4.2. *Interaction study of process variables*

Statistically significant interactive terms of adsorbent dosage-pH ($F = 163.66$; $p < 0.0001$) and adsorbent dosage-initial polyphenols concentration ($F = 16.18$; $p = 0.0007$) were highlighted through ANOVA analysis (Table S3).

Fig. 5a presents the interactive effect of adsorbent dosage-pH on polyphenols removal efficiency. Both variables pyrolysis

temperature and initial polyphenols concentration were kept constant at their central levels. According to this figure, with an adsorbent dosage of 2 g, the variation of pH from 5 to 12 yielded an increase of 23% of PC removal. However, adsorbent dosage of 15 g yielded only an increase of 10% of PC removal. This antagonist effect between dosage and pH was plausibly justified by Achak et al. (2009). These researchers argued that an adsorbent high dosage would cause the polyphenols to bind to the surface sorbent. This would result in affecting the PC affinity for the adsorbent surface. Fig. 5b depicts the interactive effect of adsorbent dosage-initial polyphenols concentration. Both variables pyrolysis temperature and pH were kept constant at their central levels. It was observed that when increasing the adsorbent dosage from 2 to 15 g with an OMW initial PC concentration of 3400 mg/L, the PC removal increased only by 10%. However, about 15% of increase in PC removal was recorded when the OMW initial PC concentration was reduced to 680 mg/L. This synergic effect between adsorbent dosage and OMW dilution can be interpreted in terms of the fact that, for non diluted OMW, the presence of many organic molecules would cause steric hindrance as well as reduce the accessibility of phenolic compounds into target sites. Hence, after OMW dilution, the uptrend in the percentage removal of polyphenols, caused by the increase of adsorbent dosage, was more noticeable. However, in industrial scale, before the requirement of OMW dilution, economic feasibility aspects need to be considered.

3.4.3. *Optimization and model validation*

Optimization was conducted to achieve the highest possible OMW polyphenols compounds removal. Results indicated that the optimum parameters were pH = 12, adsorbent dosage = 15 g/100 mL, initial OMW polyphenols concentration = 680 mg/L and pyrolysis temperature = 650 °C. The model predicted that providing these conditions would allow to achieve a PC removal of 63.16% with a desirability = 0.987.

3.5. *Adsorption isotherm*

Fig. 6 shows the isotherm data which were fitted with the following isotherms: Langmuir and Freundlich by nonlinear regression.

The nonlinear form of the Langmuir model isotherm is expressed in terms of the following equation:

$$q_e = \frac{q_{max} K_L Ce}{1 + K_L Ce} \quad (10)$$

where qe (mg/g) is the adsorbate uptake amount at equilibrium time; Ce (mg/L) is the concentration of the adsorbate at equilibrium; q_{max} (mg/g) is the maximum saturated monolayer adsorption capacity of the adsorbent and K_L (L/mg) is the Langmuir constant related to the affinity between an adsorbate and adsorbent.

In addition, dimensionless constant separation factor (R_L) was calculated using the following equation:

$$R_L = \frac{1}{1 + K_L C_0} \quad (11)$$

where C_0 is the initial concentration of the adsorbate (mg/L) and K_L is the Langmuir equilibrium constant. For a favorable equilibrium, the value of R_L is between 0 and 1. Otherwise, equilibrium is either unfavorable where $R_L > 1$; linear where $R_L = 1$ or irreversible if $R_L = 0$.

Table 4 – Isotherm parameters of Langmuir and Freundlich isotherms.

Isotherm	Parameters	
Langmuir	q_m (mg/g)	140.47
	K_L (L/mg)	$6\ 10^{-4}$
	χ^2	0.8491
	RMSE	3.0094
	R_1^2	0.9871
Freundlich	1/n	0.6594
	K_F (mg/g)/(mg/L)$^{1/n}$	0.5286
	χ^2	0.5969
	RMSE	2.4896
	R_2^2	0.9911

Freundlich (1906) proposed the nonlinear form of the Freundlich model as indicated in Eq. (12):

$$q_e = K_F C_e^{1/n} \quad (12)$$

where qe (mg/g) is the adsorbate uptake amount at equilibrium time; Ce (mg/L) is the concentration of the adsorbate at equilibrium, K_F (mg/g)/(mg/L)^n is the Freundlich constant related to the sorption capacity and n (dimensionless) is the empirical Freundlich parameter related to the intensity of sorption.

Table 4 outlines the Freundlich and Langmuir adsorption parameters evaluated from the nonlinear regression.

Even though correlation coefficients of both models were quite satisfactory (≥0.98), the value of R^2 displayed a slight privilege to the Freundlich model (R^2 = 0.9911 versus 0.9871 for the Langmuir model). Moreover, the Freundlich model exhibited lower RMSE and χ^2 values than the Langmuir model. Accordingly, Freundlich model exhibited better fit to describe polyphenols adsorption behavior onto the BC. When fitted to Langmuir model, the maximum PC sorption capacity q_{max} was equal to 140.47 mg/g. The R_L value between 0.33 and 0.78 would denote that the adsorption was favorable. When applying Freundlich equation, the value of 1/n was between 0 and 1 (0.6594), indicating favorable adsorption onto the adsorbent. Langmuir adsorption model relies on the concept that adsorption occurs at specific homogeneous surface sites within the adsorbent as well as monolayer adsorption. However, Freundlich isotherm rests upon multilayer adsorption on heterogeneous sites with non-uniform distribution of energy level. In our case, OMW adsorption on biochar fitted both models adequately. Monolayer and heterolayer phenolic compounds may exist on the adsorbent surface due to the heterogeneity of biochar surface. This observation was reported before (Achak et al., 2014, 2009).

Compared to different adsorbents for the removal of polyphenols from OMW (Table S4), BC produced in our study showed higher adsorption capacity (q_{max}) than incompletely combusted olive pomace with q_{max} of 11.4 mg/g (Stasinakis et al., 2008), or activated olive stones with q_{max} of 91.74 mg/g (Galiatsatou et al., 2002) but lower than commercial activated carbons with q_{max} of 239.17 mg/g (Senol et al., 2017).

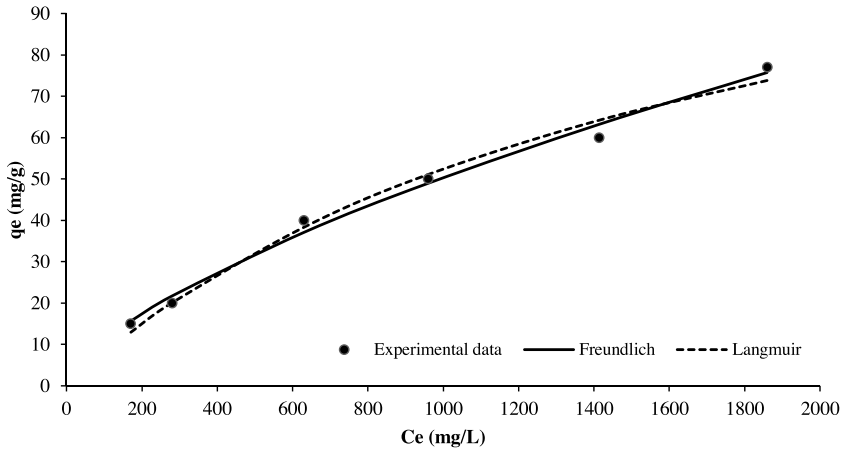

Fig. 6 – Equilibrium isotherm data for the adsorption capacity (q_e) of biochar produced at a pyrolysis temperature of 650 °C (Conditions: Temperature = 30 °C, pH = 12, adsorbent dosage = 2 g/100 mL and contact time = 24 h).

3.6. *Identification of phenolic compounds retained on BC by HPLC analysis*

To render the process of producing biochar more sustainable, it can be associated with the recovery of added-value products. In fact, BC can be considered as a low-cost adsorbent for selective separation of valuable chemicals present in OMW such as hydroxytyrosol, a substance of high demand for health and nutraceutical purposes thanks to its antioxidant activities (Bouaziz et al., 2010). For this purpose, the adsorption affinity of phenolic compounds (tyrosol and hydroxytyrosol) towards BR was evaluated. Fig. 7 highlights the HPLC analysis of phenolic monomers from pretreated OMW before and after adsorption. The results reveal that Hydroxytyrosol (238 mg/L) and tyrosol (134 mg/L) are the major phenolic compounds in pretreated OMW (Fig. 7a). Previous researchers reported that after OMW storage, both compounds proved to be the main phenolic monomers (Achak et al., 2009; Allouche et al., 2004) due to degradation processes as well as the generation of hydroxytyrosol in particular following the hydrolysis of oleuropein (Yangui et al., 2009). Compared to the chromatogram of Fig. 7a related to pretreated OMW and the one of Fig. 7b, it is easy to calculate the removal efficiency of polyphenol adsorbed on BC from OMW. In fact, by adopting the following condition: an adsorbent dosage of 5 g/100 mL, a pH of 5, a pyrolysis temperature of 450 ° C and an initial PC concentration of 3400 mg/L; a removal of 92.5% of hydroxytyrosol and 42.5% of tyrosol were recorded (Table S4). It is clear that better adsorption efficiency was observed for hydroxytyrosol, while tyrosol which has a lower polarity was less retained by adsorption as confirmed by HPLC analysis. Hence, the better efficiency of hydroxytyrosol adsorption could be attributed to the polar nature of BC which had a high (O + N)/C ratio. Indeed, Ferri et al. (2011) reported that the polar features of both resin and phenol were responsible for the adsorption efficiency of simple phenolic compounds from OMW.

Fig. 7c indicates that for non-diluted OMW and under optimal conditions (adsorbent dosage of 15 g/100 mL, a pH of 12, and a pyrolysis temperature of 650 °C), 100% of hydroxytyrosol and 77% of tyrosol removal were achieved. Under the same conditions, only 52% of total polyphenolic compounds were removed (Table S5).

Bertin et al. (2011) argued that, using weakly polar commercial resins as the solid phase extraction procedure, only 53% of total phenols, 42% of hydroxytyrosol and 67% of tyrosol were adsorbed from OMW. From this perspective, the use of BC as reported in this study may be a better option. Moreover, improvement prospects of desorption procedures by BC seem to provide promising results in terms of recovering hydroxytyrosol.

Table 5 – Chemical parameters and germination test of pretreated OMW and those of pretreated OMW after adsorption onto biochar.

Parameters	Pretreated OMW	Pretreated OMW after adsorption
COD (g/L)	47.4 ± 2.8	32.25 ± 1.6
PC (g/L)	3.4 ± 0.12	1.96 ± 0.22
Kj-N (g/L)	0.3 ± 0.06	0.22 ± 0.04
P (mg/L)	39.2 ± 1.1	31.6 ± 0.9
K (g/L)	3.12 ± 0.15	2.86 ± 0.1
Ca (mg/L)	482 ± 2.5	26.2 ± 2.8
Na (g/L)	0.735 ± 0.08	0.401 ± 0.07
Fe (g/L)	0.402 ± 0.05	0.337 ± 0.06
Mg (mg/L)	252.5 ± 1.5	61.75 ± 1.5
Mn (mg/L)	1.6 ± 0.25	1.1 ± 0.15
Zn (mg/L)	1.3 ± 0.3	0.62 ± 0.05
Cu (mg/L)	0.25 ± 0.05	0.1 ± 0.03
Germination index (%)	20 ± 1.5	68.5 ± 2.3

Data are represented by mean ± standard deviation.

3.7. *Characterization of OMW and biochar after adsorption for further reuse*

The main parameters of OMW before and after adsorption onto BC under the following conditions: an adsorbent dosage of 15 g/100 mL, a pH of 8, a PC concentration of 3400 mg/L and a pyrolysis T° of 650 °C, showed a change (Table 5). Firstly, there was a noticeable decrease of COD and PC, which alleviates the OMW pollution risk for superficial waters. OMW was rich in macro-elements (Kj-N, P, K) and essential elements for plant growth (Ca, Mg, Fe, Mn) which confirmed the potential reuse of OMW for ferti-irrigation (Mekki et al., 2013). After adsorption, there was a notable decrease in all mineral elements and particularity Na, Mg and Ca. The decrease of Na concentration may contribute to alleviate OMW salinity during soil application (Mekki et al., 2013). Likewise, the decrease in heavy metal contents such as Zn and Cu after adsorption may reduce the toxicity of this waste. Finally, a clear increase in germination index was noted. It may be due to removal of PC which

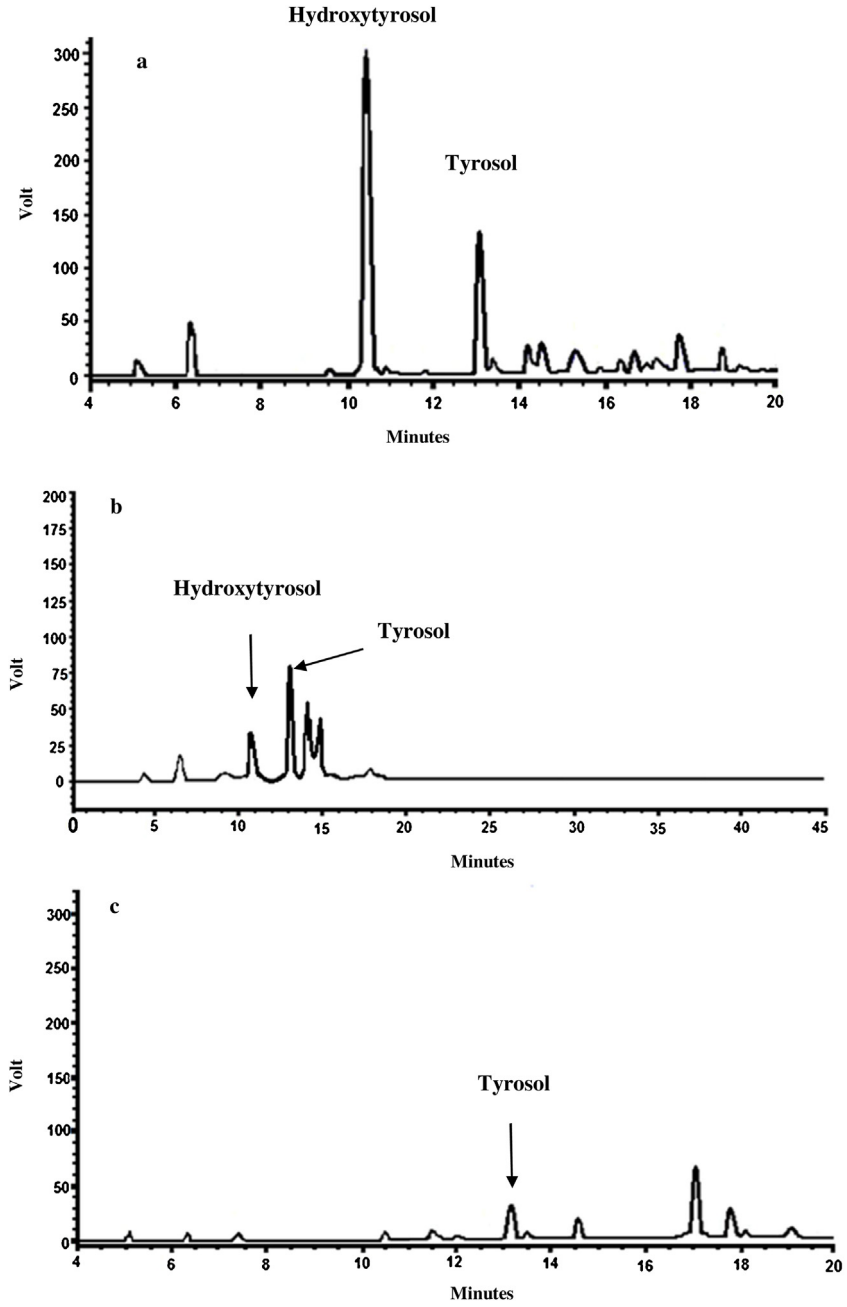

Fig. 7 – HPLC chromatograms of phenolic monomers from pretreated OMW before adsorption (a), pretreated OMW after adsorption with the following conditions (b) (adsorbent dosage = 5 g/ 100 mL, pH = 5, initial PC concentration = 3400 mg/L and pyrolysis temperature = 450 °C) and (c) (adsorbent dosage = 15 g/100 mL, pH = 12, initial PC concentration = 3400 mg/L and pyrolysis temperature = 650 °C).

were known as phytotoxic compounds (El Hajjouji et al., 2007). Hence, according to Zucconi et al. (1981), it can be concluded that the BC adsorption greatly alleviated the phytotoxic effect of OMW. Consequently, ferti-irrigation can be considered as one of the beneficial applications for OMW after adsorption.

4. Conclusion

In this study, OMSW from Tunisian evaporation ponds were transformed into biochar by pyrolysis. The results indicate that increasing carbonization temperature from 450 °C to 650 °C enhanced biochar mesoporosity. Batch adsorption experiments were conducted so as to investigate OMW polyphenols compounds removal using this biochar. Using RSM approach for optimization of the batch process parameters, pH was retained as the most highly significant variable with $p < 0.0001$. Under optimal conditions (pH of 12, initial PC of 680 mg/L, adsorbent dosage of 15 g/100 mL, pyrolysis temperature of 650 °C), a removal of 63.16 % was undertaken. A synergic effect between adsorbent dosage and OMW dilution was emphasized, which highlighted the positive effect of dilution before adsorption. However, in industrial scale, economic feasibility aspects need to be considered before the requirement of OMW dilution. The study on the equilibrium adsorption revealed that nonlinear Freundlich isotherm model was found to better describe the experimental adsorption process ($R^2 = 0.9911$), while the maximum polyphenols adsorption was 140.47 mg/g under the following conditions: a temperature of 30 °C, a pH of 12, an adsorbent dosage of 2 g/100 mL, a contact time of 24 h and polyphenols concentrations ranging from 470 to 3400 mg/L. Finally, the results showed that hydroxytyrosol appeared to have a high adsorp-

tion affinity for the biochar in view of the polar nature of biochar surface. The relevance of the present study for the industrial scale will be assessed based on pilot scale experiments. Biochar is actually being produced using an autothermal pyrolysis unit of 15 kg OMSW per cycle. The adsorption experiments will be carried out using a cascade of pilot scale adsorption columns. In industrial scale, a hybrid energy system founded on the principle of industrial symbiosis integrating pyrolysis and anaerobic digestion processes will be optimized. It can be associated with the production of hydroxytyrosol, energy carriers and fertilizer. Consequently, the required heat process can be provided through the pyrolysis process integration (that is using the volatile gases coming out from the sludge as fuel for sustaining heat production). From the point of view of social aspects, the process will limit the accumulation of the solid residue in the area and will contribute in the local development, thus improving social sustainability aspects.

Conflict of interest

The authors declare that they have no conflict of interest.

Acknowledgements

This study was supported by the project ARIMNet2 PYRODIGEST, which is funded through the ARIMNet2 2017 Joint Call by the MHESRT funding agency. The ARIMNet2 (ERANET) program received funding from the European Union's Seventh Framework Programme for research, technological development and demonstration under grant agreement no. 618127.

Appendix A. Supplementary data

Supplementary material related to this article can be found, in the online version, at doi:https://doi.org/10.1016/j.cherd.2022.02.029.

References

Abdelhadi, S.O., Dosoretz, C.G., Rytwo, G., Gerchman, Y., Azaizeh, H., 2017. Production of biochar from olive mill solid waste for heavy metal removal. Bioresour. Technol. 244, 759–767, http://dx.doi.org/10.1016/j.biortech.2017.08.013.

Achak, M., Hafidi, A., Mandi, L., Ouazzani, N., 2014. Removal of phenolic compounds from olive mill wastewater by adsorption onto wheat bran. Desalin. Water Treat. 52, 2875–2885, http://dx.doi.org/10.1080/19443994.2013.819166.

Achak, M., Hafidi, A., Ouazzani, N., Sayadi, S., Mandi, L., 2009. Low cost biosorbent "banana peel" for the removal of phenolic compounds from olive mill wastewater: kinetic and equilibrium studies. J. Hazard. Mater. 166, 117–125, http://dx.doi.org/10.1016/j.jhazmat.2008.11.036.

Ahmaruzzaman, M., Sharma, D.K., 2005. Adsorption of phenols from wastewater. J. Colloid Interface Sci. 287, 14–24, http://dx.doi.org/10.1016/j.jcis.2005.01.075.

Aktas, E.S., Imre, S., Ersoy, L., 2001. Characterization and lime treatment of olive mill wastewater. Water Res. 35, 2336–2340, http://dx.doi.org/10.1016/S0043-1354(00)00490-5.

Aliakbarian, B., Casazza, A.A., Perego, P., 2015. Kinetic and isotherm modelling of the adsorption of phenolic compounds from olive mill wastewater onto activated carbon. Food Technol. Biotechnol. 53, 207–214, http://dx.doi.org/10.17113/ftb.53.02.15.3790.

Allouche, N., Fki, I., Sayadi, S., 2004. Toward a high yield recovery of antioxidants and purified hydroxytyrosol from olive mill wastewaters. J. Agric. Food Chem. 52, 267–273, http://dx.doi.org/10.1021/jf034944u.

APHA, 2012. Standard Methods for the Examination of Water and Wastewater, 22th ed. Am. Public Heal. Assoc. Washingt., DC, USA.

Bajpai, S., Gupta, S.K., Dey, A., Jha, M.K., Bajpai, V., Joshi, S., Gupta, A., 2012. Application of Central Composite Design approach for removal of chromium (VI) from aqueous solution using weakly anionic resin: modeling, optimization, and study of interactive variables. J. Hazard. Mater. 227–228, 436–444, http://dx.doi.org/10.1016/j.jhazmat.2012.05.016.

Bertin, L., Ferri, F., Scoma, A., Marchetti, L., Fava, F., 2011. Recovery of high added value natural polyphenols from actual olive mill wastewater through solid phase extraction. Chem. Eng. J. 171, 1287–1293, http://dx.doi.org/10.1016/j.cej.2011.05.056.

Bouaziz, M., Feki, I., Ayadi, M., Jemai, H., Sayadi, S., 2010. Stability of refined olive oil and olive-pomace oil added by phenolic compounds from olive leaves. Eur. J. Lipid Sci. Technol. 112, 894–905, http://dx.doi.org/10.1002/ejlt.200900166.

Bouzid, J., Elouear, Z., Ksibi, M., Feki, M., Montiel, A., 2008. A study on removal characteristics of copper from aqueous solution by sewage sludge and pomace ashes. J. Hazard. Mater. 152, 838–845, http://dx.doi.org/10.1016/j.jhazmat.2007.07.092.

C.O.I, 2017. Conseil oleicole international (COI). Journal-officiel-du-conseil-oleicole-international, pp. 124.

Cantrell, K.B., Hunt, P.G., Uchimiya, M., Novak, J.M., Ro, K.S., 2012. Impact of pyrolysis temperature and manure source on physicochemical characteristics of biochar. Bioresour. Technol. 107, 419–428, http://dx.doi.org/10.1016/j.biortech.2011.11.084.

Chen, B., Chen, Z., 2009. Sorption of naphthalene and 1-naphthol by biochars of orange peels with different pyrolytic temperatures. Chemosphere 76, 127–133, http://dx.doi.org/10.1016/j.chemosphere.2009.02.004.

Dąbrowski, A., Podkościelny, P., Hubicki, Z., Barczak, M., 2005. Adsorption of phenolic compounds by activated carbon — a critical review. Chemosphere 58, 1049–1070, http://dx.doi.org/10.1016/j.chemosphere.2004.09.067.

Doula, M.K., Moreno-Ortego, J.L., Tinivella, F., Inglezakis, V.J., Sarris, A., Komnitsas, K., 2017. Olive mill waste: recent advances for the sustainable development of olive oil industry. In: Olive Mill Waste: Recent Advances for Sustainable Management. Elsevier Inc., http://dx.doi.org/10.1016/B978-0-12-805314-0.00002-9.

Ducom, G., Gautier, M., Pietraccini, M., Tagutchou, J.P., Lebouil, D., Gourdon, R., 2020. Comparative analyses of three olive mill solid residues from different countries and processes for energy recovery by gasification. Renew. Energy 145, 180–189, http://dx.doi.org/10.1016/j.renene.2019.05.116.

Ekpete, O.A., Horsfall, J., Tarawou, T., 2010. Potential of fluted and commercial activated carbons for phenol removal in aqueous systems. J. Eng. Appl. Sci. 5, 39–47.

El-Gohary, F.A., Badawy, M.I., El-Khateeb, M.A., El-Kalliny, A.S., 2009. Integrated treatment of olive mill wastewater (OMW) by the combination of Fenton's reaction and anaerobic treatment. J. Hazard. Mater. 162, 1536–1541, http://dx.doi.org/10.1016/j.jhazmat.2008.06.098.

El Hajjouji, H., Fakharedine, N., Ait Baddi, G., Winterton, P., Bailly, J.R., Revel, J.C., Hafidi, M., 2007. Treatment of olive mill waste-water by aerobic biodegradation: an analytical study using gel permeation chromatography, ultraviolet-visible and Fourier transform infrared spectroscopy. Bioresour. Technol. 98, 3513–3520, http://dx.doi.org/10.1016/j.biortech.2006.11.033.

FAOSTAT, 2014. Food and Agriculture Organization of the United Nations.

Ferri, F., Bertin, L., Scoma, A., Marchetti, L., Fava, F., 2011. Recovery of low molecular weight phenols through solid-phase extraction. Chem. Eng. J. 166, 994–1001, http://dx.doi.org/10.1016/j.cej.2010.11.090.

Freundlich, H., 1906. Über die adsorption in lö sungen. Z Phys. Chem. 57, 385–471.

Galiatsatou, P., Metaxas, M., Arapoglou, D., Kasselouri-Rigopoulou, V., 2002. Treatment of olive mill waste

water with activated carbons from agricultural by-products. Waste Manag. 22, 803–812, http://dx.doi.org/10.1016/S0956-053X(02)00055-7.
Garcia-Castello, E., Cassano, A., Criscuoli, A., Conidi, C., Drioli, E., 2010. Recovery and concentration of polyphenols from olive mill wastewaters by integrated membrane system. Water Res. 44, 3883–3892, http://dx.doi.org/10.1016/j.watres.2010.05.005.
Habib Dakhil, I., 2013. Removal of phenol from industrial wastewater using sawdust. Res. Inven. Int. J. Eng. Sci. 3, 25–31.
Hafidi, M., Amir, S., Revel, J.C., 2005. Structural characterization of olive mill waster-water after aerobic digestion using elemental analysis, FTIR and 13C NMR. Process Biochem. 40, 2615–2622, http://dx.doi.org/10.1016/j.procbio.2004.06.062.
Haghseresht, F., Nouri, S., Finnerty, J.J., Lu, G.Q., 2002. Effects of surface chemistry on aromatic compound adsorption from dilute aqueous solutions by activated carbon. J. Phys. Chem. B 106, 10935–10943, http://dx.doi.org/10.1021/jp025522a.
Han, R., Zou, W., Zhang, Z., Shi, J., Yang, J., 2006. Removal of copper(II) and lead(II) from aqueous solution by manganese oxide coated sand. I. Characterization and kinetic study. J. Hazard. Mater. 137, 384–395, http://dx.doi.org/10.1016/j.jhazmat.2006.02.021.
Hanandeh, A. El, Abu-Zurayk, R.A., Hamadneh, I., Al-Dujaili, A.H., 2016. Characterization of biochar prepared from slow pyrolysis of Jordanian olive oil processing solid waste and adsorption efficiency of Hg2+ ions in aqueous solutions. Water Sci. Technol. 74, 1899–1910, http://dx.doi.org/10.2166/wst.2016.378.
Hmid, A., Mondelli, D., Fiore, S., Fanizzi, F.P., Al Chami, Z., Dumontet, S., 2014. Production and characterization of biochar from three-phase olive mill waste through slow pyrolysis. Biomass Bioenergy 71, 330–339, http://dx.doi.org/10.1016/j.biombioe.2014.09.024.
Ho, Y.S., McKay, G., 1999. Pseudo-second order model for sorption processes. Process Biochem. 34, 451–465, http://dx.doi.org/10.1016/S0032-9592(98)00112-5.
Hu, X., Zhang, X., Ngo, H.H., Guo, W., Wen, H., Li, C., Zhang, Y., Ma, C., 2020. Comparison study on the ammonium adsorption of the biochars derived from different kinds of fruit peel. Sci. Total Environ. 707, 135544, http://dx.doi.org/10.1016/j.scitotenv.2019.135544.
Khoufi, S., Aloui, F., Sayadi, S., 2009. Pilot scale hybrid process for olive mill wastewater treatment and reuse. Chem. Eng. Process. Process Intensif. 48, 643–650, http://dx.doi.org/10.1016/j.cep.2008.07.007.
Khoufi, S., Aloui, F., Sayadi, S., 2006. Treatment of olive oil mill wastewater by combined process electro-Fenton reaction and anaerobic digestion. Water Res. 40, 2007–2016, http://dx.doi.org/10.1016/j.watres.2006.03.023.
Lawal, A.A., Hassan, M.A., Ahmad Farid, M.A., Yasim-Anuar, T.A.T., Mohd Yusoff, M.Z., Zakaria, M.R., Roslan, A.M., Mokhtar, M.N., Shirai, Y., 2020. One-step steam pyrolysis for the production of mesoporous biochar from oil palm frond to effectively remove phenol in facultatively treated palm oil mill effluent. Environ. Technol. Innov. 18, 100730, http://dx.doi.org/10.1016/j.eti.2020.100730.
Li, W., Amin, F.R., Fu, Y., Zhang, H., He, Y., Huang, Y., Liu, G., Chen, C., 2018. Effects of temperature, heating rate, residence time, reaction atmosphere, and pressure on biochar properties. J. Biobased Mater. Bioenergy 13, 1–10, http://dx.doi.org/10.1166/jbmb.2019.1789.
Lima, E.C., Royer, B., Vaghetti, J.C.P., Brasil, J.L., Simon, N.M., dos Santos, A.A., Pavan, F.A., Dias, S.L.P., Benvenutti, E.V., da Silva, E.A., file///C/Users/Asus/Desktop/Refus/soumission 2007. Adsorption of Cu(II) on Araucaria angustifolia wastes: determination of the optimal conditions by statistic design of experiments. Chem. Des. Hazard. Mater. 140, 211–220, http://dx.doi.org/10.1016/j.jhazmat.2006.06.073.
Liu, W.J., Zeng, F.X., Jiang, H., Zhang, X.S., 2011. Preparation of high adsorption capacity bio-chars from waste biomass. Bioresour. Technol. 102, 8247–8252, http://dx.doi.org/10.1016/j.biortech.2011.06.014.
Martín-Lara, M.A., Pérez, A., Vico-Pérez, M.A., Calero, M., Blázquez, G., 2019. The role of temperature on slow pyrolysis of olive cake for the production of solid fuels and adsorbents. Process Saf. Environ. Prot. 121, 209–220, http://dx.doi.org/10.1016/j.psep.2018.10.028.
McNamara, C.J., Anastasiou, C.C., O'Flaherty, V., Mitchell, R., 2008. Bioremediation of olive mill wastewater. Int. Biodeterior. Biodegrad. 61, 127–134, http://dx.doi.org/10.1016/j.ibiod.2007.11.003.
Mekki, A., Dhouib, A., Sayadi, S., 2013. Review: effects of olive mill wastewater application on soil properties and plants growth. Int. J. Recycl. Org. Waste Agric. 2, http://dx.doi.org/10.1186/2251-7715-2-15.
Mohammed, N.A.S., Abu-Zurayk, R.A., Hamadneh, I., Al-Dujaili, A.H., 2018. Phenol adsorption on biochar prepared from the pine fruit shells: equilibrium, kinetic and thermodynamics studies. J. Environ. Manage. 226, 377–385, http://dx.doi.org/10.1016/j.jenvman.2018.08.033.
Mondal, S., Bobde, K., Aikat, K., Halder, G., 2016. Biosorptive uptake of ibuprofen by steam activated biochar derived from mung bean husk: equilibrium, kinetics, thermodynamics, modeling and eco-toxicological studies. J. Environ. Manage. 182, 581–594, http://dx.doi.org/10.1016/j.jenvman.2016.08.018.
Parsa, M., Nourani, M., Baghdadi, M., Hosseinzadeh, M., Pejman, M., 2019. Biochars derived from marine macroalgae as a mesoporous by-product of hydrothermal liquefaction process: characterization and application in wastewater treatment. J. Water Process Eng. 32, 100942, http://dx.doi.org/10.1016/j.jwpe.2019.100942.
Peng, X., Ye, L.L., Wang, C.H., Zhou, H., Sun, B., 2011. Temperature- and duration-dependent rice straw-derived biochar: characteristics and its effects on soil properties of an Ultisol in southern China. Soil Tillage Res. 112, 159–166, http://dx.doi.org/10.1016/j.still.2011.01.002.
Petrotos, K.B., Kokkora, M.I., Gkoutsidis, P.E., Leontopoulos, S., 2016. A comprehensive study on the kinetics of olive mill wastewater (OMWW) polyphenols adsorption on macroporous resins. Part II. The case of Amberlite FPX66 commercial resin. Desalin. Water Treat. 57, 20631–20638, http://dx.doi.org/10.1080/19443994.2015.1111820.
Quast, K., 2018. Direct measurement of oleate adsorption on hematite and its consequences for flotation. Miner. Eng. 118, 122–132, http://dx.doi.org/10.1016/j.mineng.2017.12.011.
Sanginés, P., Domínguez, M.P., Sánchez, F., San Miguel, G., 2015. Slow pyrolysis of olive stones in a rotary kiln: chemical and energy characterization of solid, gas, and condensable products. J. Renew. Sustain. Energy 7, http://dx.doi.org/10.1063/1.4923442.
Sayadi, S., Allouche, N., Jaoua, M., Aloui, F., 2000. Detrimental effects of high molecular-mass polyphenols on olive mill wastewater biotreatment. Process Biochem. 35, 725–735, http://dx.doi.org/10.1016/S0032-9592(99)00134-X.
Senol, A., Hasdemir, M., Hasdemir, B., Kurdaş, 2017. Adsorptive removal of biophenols from olive mill wastewaters (OMW) by activated carbon: mass transfer, equilibrium and kinetic studies. Asia-Pacific J. Chem. Eng. 12, 128–146, http://dx.doi.org/10.1002/apj.2060.
Stasinakis, A.S., Elia, I., Petalas, A.V., Halvadakis, C.P., 2008. Removal of total phenols from olive-mill wastewater using an agricultural by-product, olive pomace. J. Hazard. Mater. 160, 408–413, http://dx.doi.org/10.1016/j.jhazmat.2008.03.012.
Tran, H.N., Chao, H.P., You, S.J., 2018. Activated carbons from golden shower upon different chemical activation methods: Synthesis and characterizations. Adsorpt. Sci. Technol. 36, 95–113, http://dx.doi.org/10.1177/0263617416684837.
Tsagaraki, E., Lazarides, H.N., Petrotos, K.B., 2007. Olive mill wastewater treatment. In: Utilization of By-Products and Treatment of Waste in the Food Industry., http://dx.doi.org/10.1007/978-0-387-35766-9_8.
Xiaoli, C., Youcai, Z., 2006. Adsorption of phenolic compound by aged-refuse. J. Hazard. Mater. 137, 410–417, http://dx.doi.org/10.1016/j.jhazmat.2006.02.015.
Yang, T., Lua, A.C., 2003. Characteristics of activated carbons prepared from pistachio-nut shells by physical activation. J.

Colloid Interface Sci. 267, 408–417, http://dx.doi.org/10.1016/S0021-9797(03)00689-1.
Yangui, T., Dhouib, A., Rhouma, A., Sayadi, S., 2009. Potential of hydroxytyrosol-rich composition from olive mill wastewater as a natural disinfectant and its effect on seeds vigour response. Food Chem. 117, 1–8, http://dx.doi.org/10.1016/j.foodchem.2009.03.069.
Zhang, G., Zhang, Q., Sun, K., Liu, X., Zheng, W., Zhao, Y., 2011. Sorption of simazine to corn straw biochars prepared at different pyrolytic temperatures. Environ. Pollut. 159, 2594–2601, http://dx.doi.org/10.1016/j.envpol.2011.06.012.
Zucconi, et al., 1981. Evaluating toxicity of immature compost. Biocycle 22, 54–57.